Adsorption of Polyampholytes to Charged Surfaces

Malek O. Khan,* Torbjörn Åkesson, and Bo Jönsson

Theoretical Chemistry, Chemical Center, Lund University, POB 124, SE-22100 Lund, Sweden

Received August 16, 2000; Revised Manuscript Received February 26, 2001

ABSTRACT: The adsorption of flexible polyampholytes to charged surfaces has been investigated. The electrostatic interactions are included in a mean-field manner, while the chain connectivity is treated by Metropolis Monte Carlo (MC) simulations. For large enough surface charge densities, adsorption is found both for neutral polyampholytes and for polyampholytes carrying the same net charge as the surfaces. The simulation results are used to check the reliability of previously proposed analytical theories. The exponents predicted in those scaling relations are not reproduced by MC simulations. The simulations show that the size of the adsorbed polyampholyte initially grows with increasing surface charge density, but for sufficiently charged surfaces it reaches a maximum and starts to decrease. This general behavior is qualitatively captured by scaling arguments. The MC simulations do not bear any evidence for the existence of three disparate regimes where the polyampholyte adsorbs in different conformations.

1. Introduction

Charged polyions are an important subset of polymers comprising biopolymers such as DNA, RNA, and proteins and also synthetic species, which are important in practical applications. Polyelectrolytes have been extensively studied by experimental and theoretical means. Much less is known about polyampholytes, which are polymers containing both positively and negatively charged chain segments, although a recent review on polyampholytes is available.[1]

The overall topology of a polyampholyte is important for its conformational properties in solution. Polyampholytes with a net charge are dominated by the polyelectrolyte effect; i.e., a strong repulsion between like-charged monomers stretches the chain, and these chains dissolve even in solvents that are poor for the polymer backbone. For neutral polyampholytes the charge sequence is important which has been shown in experiments,[2] simulations,[3−5] and analytical theories.[6,7] Narrow distributions, where the extreme is alternating charges, lead to a swollen chain that dissolves readily, while polyampholytes with broad charge distributions tend to collapse and precipitate.

For ensembles of polyampholytes with random distributions of charges there exists a net-charge threshold for which the polyampholytes collapses $|f_+ - f_-| < 1/\sqrt{N}$.[8−10] Here f_+ is the fraction of positive charges, f_- is the fraction of negative charges, and N is the number of monomers. Thus, the longer the chain, the lower is the threshold for collapse.

Less is known about the adsorption behavior of polyampholytes to charged surfaces and colloidal particles, although the importance of understanding protein and polyampholyte adsorption for controlling emulsion stability and rheology is well documented.[11] Many technological processes such as wastewater treatment, flotation, paper production, etc., are closely connected with adsorption phenomena, and polyampholytes are widely used in the food, the photographic, and the pharmaceutical industries as stabilizers and modifiers of interfacial properties. Adsorption of ampholytic proteins plays a key role in many biological processes, e.g. drug delivery, biocompatibility, and blood coagulation.

In recent years, experiments[12] and also analytical theories[13−16] concerning the complexation behavior of polyampholytes have been presented, and the main conclusion is that neutral polyampholytes and even polyampholytes with a net charge opposite to the wall charge adsorb to the wall.

In the present work, the adsorption behavior of a polyampholyte to a charged surface is investigated with numerical tools. While the charged surface and its counterions throughout this work will be treated in a mean-field manner, the chain properties will be treated with Monte Carlo (MC) simulations. For short chains or when the intrachain electrostatics are weak, the polyampholytes will take on Gaussian conformations in the absence of an external electrical field. In other words, when the electrostatic interactions between two monomers are smaller than kT (k is the Boltzmann constant and T is the absolute temperature), the chain entropy will dominate the conformational behavior. The present simulations take advantage of the fact that the systems studied are in this so-called weak coupling regime.[9,5,10] (For stronger coupling the polyampholyte would form a globule and precipitate.) This permits the use of a simplified model where the intrachain electrostatic interactions are neglected, which decreases the computing time with an order of magnitude. Comparisons with simulations that include the intrachain electrostatics are included to validate the simplified model.

The simulations performed without intrachain electrostatics give an opportunity for comparison with some of the analytical theories developed by Dobrynin et al.[14] and Netz and Joanny.[16] The theories of interest here are valid in the weak coupling regime and predict that the adsorption behavior for a single polyampholyte is due to the fact that the field from the charged wall polarizes the polyampholyte which is attracted to the charged wall. Adsorption is found for neutral polyampholytes and for polyampholytes with the same net charge as the wall as long as the attraction, due to the polarization of the chain, is stronger than the net charge repulsion.

* Corresponding author. E-mail Malek.Khan@teokem.lu.se.

10.1021/ma001437u CCC: $20.00
Published on Web 05/03/2001

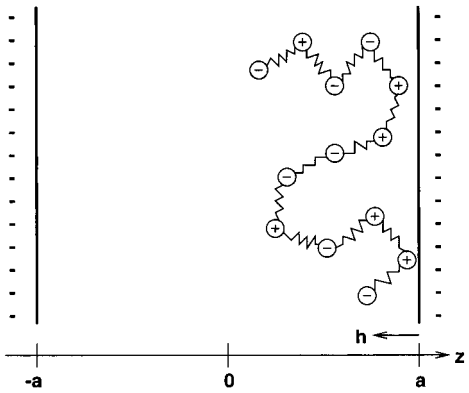

Figure 1. A schematic figure of the model used in the simulations. The walls are perpendicular to the *z*-axis, and $z = 0$ is in the middle of the two surfaces which are a distance $2a$ apart. Note that in the simulations performed the two walls are very far from each other which is not reflected by the figure.

Table 1. Scaling Results According to the Mean-Field Approaches by Netz and Joanny and by Dobrynin et al. from Which the Naming of the Different Regions Is Adapted

λ_{GC}	$\langle z^2\rangle^{1/2}$
$\lambda_{GC} > bNf^{1/2}/2\pi$	no adsorption
$\lambda_{GC} > \langle z^2\rangle^{1/2}$	$b^2N^{3/2}\lambda_{GC}^{-1}f^{1/2}$ (pole)
$\lambda_{GC} < \langle z^2\rangle^{1/2}$	λ_{GC} (fence)
$\lambda_{GC} < bf^{-1/2}/2\pi$	$bf^{-1/2}$ (pancake)

The scaling relations predicted by the theoretical work in this area,[14,16] see Table 1 (in which λ_{GC} is the Gouy−Chapman length defined in eq 3, f is the fraction of charged monomers, b is the bond length, and $\langle z^2\rangle^{1/2}$ is the z-component of the end-to-end distance), claim that the adsorption behavior can be divided into three regimes depending on the surface charge density. The pole regime (for low surface charge) where the polyampholyte adsorbs in a single stretched coil of vertical size smaller than the Gouy−Chapman length, the fence regime where the polyampholyte adsorbs in multiple blobs with a vertical size comparable to the Gouy−Chapman length, and the pancake regime (for high surface charge) where the polyampholyte adsorbs in multiple blobs of size $bf^{-1/2}$.

We will now continue in section 2 by introducing the numerical methods used. A presentation of the results is given in section 3 together with a discussion of the validity of analytical theories. Finally in section 4, conclusions from the present study are summarized.

2. Computer Simulations

The system of interest is a polyampholyte in between two charged walls, and a schematic figure of the model is depicted in Figure 1.

2.1. The Mean Field. Throughout this work, the potential originating from the charged surfaces and its counterions is treated in a mean-field approximation. The surfaces and counterions give rise to an effective potential[17,18]

$$V_p(z) = \frac{kT}{Ze}\ln\left[\cos^2\left(\frac{sz}{a}\right)\right] \tag{1}$$

where z is the distance from the midplane between the surfaces, a is half the surface−surface distance, and Ze is the counterion charge. Only monovalent counterions will be considered; hence, Z will be put to unity henceforth. The parameter s can be found from

$$s\tan s = -\frac{\sigma e a}{2kT\epsilon_r\epsilon_0} = -\frac{a}{\lambda_{GC}} \tag{2}$$

by iteration. In eq 2, the surface charge σ is introduced together with the dielectric permittivity $\epsilon_r\epsilon_0$. The last equality defines the so-called Gouy−Chapman length λ_{GC} as

$$\lambda_{GC} = \frac{e}{2\pi l_B\sigma} \tag{3}$$

where l_B is the Bjerrum length $l_B = e^2/4\pi\epsilon_0\epsilon_r kT$ and has a value of 7.14 Å for water at room temperature. The Gouy−Chapman length is the distance from the surface at which the electrostatic interaction between a monovalent ion and the surface will be in the order of the thermal energy kT, and the Bjerrum length is the distance at which the electrostatic interaction between two monovalent particles equals kT. The Gouy−Chapman length becomes smaller with increasing surface charge density, as seen in eq 3, which also means that the potential varies faster. This fact is important for the thickness of the adsorbed polyampholyte. Typical values for the Gouy−Chapman length are the following: mica, ∼1 Å; DNA, ∼5 Å; biological membranes, ∼5 Å; weakly charged proteins, ∼100 Å.

2.2. Model Systems. In the simulations the polyampholyte is made up of charged point particles connected by harmonic springs. (When intrachain electrostatics are included, charged hard spheres are used instead.) The macromolecule is enclosed between two negatively charged surfaces, represented by infinite plane walls with a uniform charge density σ. Since the main focus in this work is on adsorption of a polyampholyte, the surfaces are kept widely apart to ensure that the chain only adsorbs to one wall at a time. The solvent only enters via the dielectric constant $\epsilon_r = 78.7$, valid for water at a temperature $T = 298$ K. In the following two models, the potential originating from the charged surface is treated in the mean-field approximation described above; i.e., the counterions are not modeled explicitly but rather by modifying the wall potential into an effective potential described by eq 1. The chain is described in two different levels of approximation, with and without intrachain electrostatics.

2.3. Monte Carlo without Intrachain Electrostatics. In this model it is assumed that the equilibrium conformation (when disregarding the walls) of the chains is Gaussian. To model a Gaussian chain, the monomers building up the chain do not interact electrostatically with each other but only with the mean-field potential originating from the adsorbing surface and its counterions. Thus, the total energy for a polyampholyte built up by N monomers is given by

$$E_0 = \sum_{i=1}^{N}\nu_i eV_p(z_i) + \sum_{i=1}^{N-1}\frac{K}{2}(|\mathbf{r}_i - \mathbf{r}_{i+1}|^2) \tag{4}$$

where ν_i is the valence (±1 or 0) and $\mathbf{r}_i$ is the position of monomer i. K is the spring constant, chosen to $K = 13.6 \times 10^{-3}$ N/m, which sets the average monomer−monomer distance to $b \approx 10$ Å at room temperature. This simple model is suitable for comparisons with the analytical theories presented in the Introduction.[14,16]

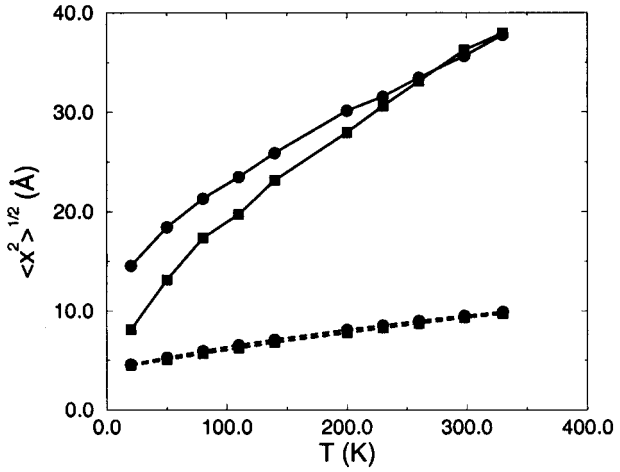

Figure 2. Solid lines show the *x*-component of the end-to-end distance, and the dashed lines show the nearest bead distances as a function of temperature. Squares are used for the model which includes intrachain electrostatic interactions and circles for the model without those interactions. The simulations have been carried out for chains with $N = 40$.

2.4. Monte Carlo with Intrachain Electrostatics Included. Here the intrachain electrostatics are included while the wall and counterions are still modeled in the mean-field approximation resulting in

$$E = E_0 + \sum_{i<j}^{N} \frac{\nu_i \nu_j e^2}{4\pi\epsilon_r\epsilon_0|\mathbf{r}_i - \mathbf{r}_j|} + \sum_{i<j}^{N} u_{ij}^{hc}(r_{ij}) \qquad (5)$$

where u_{ij}^{hc}, the hard-core term, now is included as

$$u_{ij}^{hc}(r_{ij}) = \begin{cases} 0, & |\mathbf{r}_i - \mathbf{r}_j| \geq d \\ \infty, & |\mathbf{r}_i - \mathbf{r}_j| < d \end{cases} \qquad (6)$$

with $d = 4$ Å being the particle diameter.

2.5. Methods. The Monte Carlo (MC) simulations of the model systems are performed in the canonical ensemble with the traditional Metropolis algorithm.[19,20] The monomers are moved one at a time, and the new energies are computed according to eq 4 or 5. The time to achieve good statistics is hugely different for the two methods outlined above. The simulations without intrachain electrostatics took minutes while the inclusion of the intrachain electrostatics increased the simulation time needed to hours on a powerful workstation.

3. Results and Discussion

The simplified polyampholytes studied in this work are not intended to mimic actual experimentally realizable polymers; rather, the goal is to point out the qualitative behavior of polyampholytes, near a charged surface. The importance of intrachain electrostatics can be inferred from a comparison of the *x*-component of the end-to-end distance $\langle x^2\rangle^{1/2}$calculated with and without intrachain electrostatics, since there is no external field in the *x*-direction. For low temperatures, i.e., strong coupling, the two approaches may differ by a factor of 2, but at room temperature the $\langle x^2\rangle^{1/2}$ obtained in the simulations are indistinguishable (see Figure 2).[5,10,21] These findings support the use of the more simple and computationally appealing approach, eq 4. It is also interesting to note that the average monomer−monomer distance *b* is the same in both approaches.[5]

Another restriction is that almost all the chains studied here are fully charged. For a realistic polyampholyte the proportion of charged monomers will be smaller than one ($f < 1$). But, the qualitative behaviors of chains with $f < 1$ and $f = 1$ are very much alike, which will soon become evident. By using fully charged polyampholytes, it is somewhat easier to classify the different sequences.

A broad spectrum of methods has been developed for investigating the nonrandomness of sequences in the folding of proteins into specific ground states (see e.g. Irbäck et al.[22] and references therein). For the electrostatic interactions considered here, there exists no unique ground state, and only a simple classification scheme will be used which will provide the general trend. One way of characterizing the sequence is to define a local charge correlation parameter (for a neutral chain where every monomer has a charge) as

$$h_{corr} = \frac{\sum_{i=1}^{N-1} \nu_i \nu_{i+1}}{N - 2} \qquad (7)$$

This parameter is constructed so that $h_{corr} = 1$ for a diblock polyampholyte, $h_{corr} = -1$ for a perfectly alternating, and $h_{corr} = 0$ for a totally random chain.

Obviously, when discussing the adsorption of a polyampholyte to a charged surface, features regarding both the electric double layer and the charged polymer are of importance. The number of parameters (length scales) is large and includes among others the Bjerrum length, the Gouy−Chapman length, the chain length, and the hard core radius. Here we will focus on a dilute polyampholyte solution and anticipate that for a sufficiently long chain a variation of λ_{GC} and the charge sequence will reveal most of the physical properties relevant for a real system.

3.1. Neutral Polyampholytes. The monomer distribution $\rho_m(h)$, where $h = a - z$ is the distance to the wall (see Figure 1), for polyampholytes with different charge sequences is shown in Figure 3. It seems clear that all but the alternating chain are drawn to the wall. The chains try to orient its positive monomers to the negative wall and keep its negative parts as far away as possible. Naturally, this is easiest for the diblock chain and hardly possible at all for the alternating chain, for which the two distribution curves (for positive and negative monomers) are almost identical. The charges on the random chain, with less charge fraction $f = 0.1$, can adjust better to the field from the wall, and the higher flexibility of these charges accounts for a tail far from the wall. Still there are only small qualitative differences between this chain and the other random chains, and all of them are more or less attracted to the wall.

Another way of visualizing the adsorption to the charged surface is to measure the fraction of chains whose center of mass resides within an undisturbed chain length from the wall, $h_0 = b\sqrt{N-1}$. The adsorption Γ is thus defined as

$$\Gamma = \int_0^{h_0} \frac{\rho(h)}{\rho_{av} h_0}\, dh \qquad (8)$$

where $\rho(h)$ is the center-of-mass distribution function and ρ_{av} is the average density. The range of Γ is $0 < \Gamma < a/h_0$, and if $\Gamma > 1$, the chain is considered to be adsorbed. The rather arbitrary choice of cutoff length

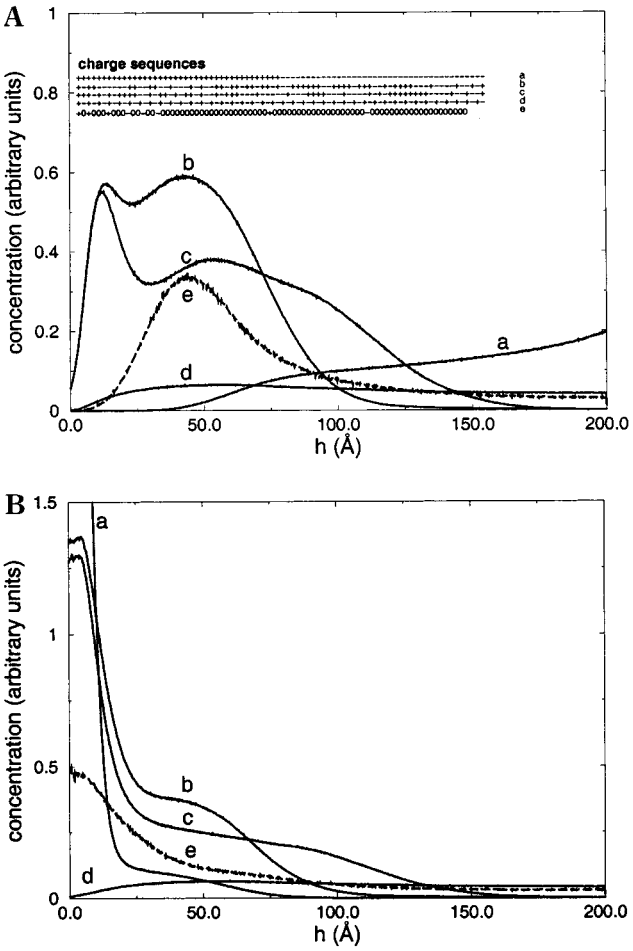

Figure 3. Distribution function for the (A) negative and (B) positive monomers, of polyampholytes with different charge sequences, near a negatively charged wall. The solid lines corresponds to $f = 1$ and the dashed to $f = 0.1$. The amplitudes of the latter chain has been multiplied by 10, since the charge concentration is 1/10 of the other chains. The simulations have been carried out for chains with $N = 80$. The surface charge was one charge per 400 Å^2, which corresponds to a Gouy−Chapman parameter $\lambda = 8.9$ Å. Also in the figure are the charge sequences of the polyampholytes. Note that the two polyampholytes with $h_{corr} = 0$ have different charge sequences and that the scales of (A) and (B) do not coincide.

h_0 has been checked, and the qualitative results stand firm. By defining a single polyampholyte as adsorbed if $h < h_0$, it is possible to distinguish the properties of the adsorbed chains from the properties of the nonadsorbed. The different mean values, such as $\langle z^2 \rangle$, are thus averaged over the adsorbed chains only. This implies that when averaging over chains with different charge sequences, those with a greater tendency to adsorb will give a larger contribution to the mean values.

Alternatively, the adsorption can be defined as the proportion of monomers inside a certain cutoff length. The actual numbers are sensitive to the choice of cutoff length, but the qualitative behavior is the same for 5, 10, 15, and 20 Å. Clearly, the definition of adsorption is somewhat arbitrary, but for sensible choices the qualitative behavior is not much altered.

In Figure 3 the adsorptions for different charge sequences are shown. The diblock polyampholyte adsorbs to a great extent, with the oppositely charged half close to the wall and the like charged half dangling out from the wall. The alternating chain adsorbs very little since this chain is hardly polarized and prefers the bulk

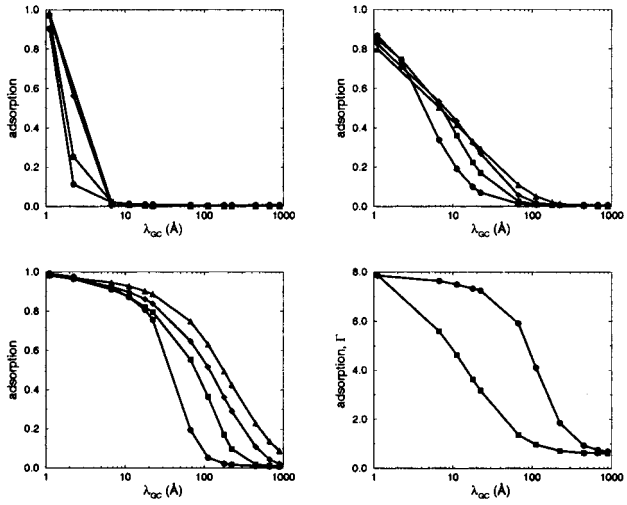

Figure 4. Adsorption of polyampholytes, with different N and f, to walls with surface charges between 1/50 e/Å^2 and 1/40 000 e/Å^2(1.1 Å $< \lambda_{GC} <$ 890 Å). In the first three graphs the adsorption is defined as the proportion of positive monomers within 20 Å from the negative wall. (A), (B), and (C) correspond to different charge sequences; (A) $h_{corr} = -1$, (B) $h_{corr} \approx 0$, and (C) $h_{corr} = 1$. The results in (B) are averaged over 100 different random sequences. The different chain lengths are $N = 20$ (circles), $N = 40$ (squares), $N = 80$ (diamonds), and $N = 160$ (triangles). (D) Adsorption, defined in eq 8, as a function of the Gouy−Chapman length for different f; $f = 1.0$ (circles) and $f = 0.1$ (squares). For every f, 100 chains with random sequences have been used, each with $N = 160$ and $b \approx 10$ Å.

before the charged surface. The different random chains fit somewhere in between. For long polyampholytes the number of chains with $h_{corr} \approx 0$ will be dominating due to the high degeneracy of these chains, and their adsorption behavior can be expected to resemble each other as can be seen for the two chains in Figure 3 with $h_{corr} = 0$.

From the discussion in the Introduction it is clear that the Gouy−Chapman length is an interesting parameter. Here we will investigate λ_{GC} by changing the surface charge concentration σ, in a broad range from 1 charge per 50 Å^2 to 1 charge per 40 000 Å^2, which means a variation in λ_{GC} of 1 to 800 Å, well beyond most real systems. In Figure 4A−C the adsorptions for alternating, random, and diblock chains are shown. The general behavior is the same for all the investigated chains, with high adsorption for low λ_{GC} and with a decreasing adsorption with increasing λ_{GC}. Notably, it is possible for the alternating chain to adsorb only at very high surface charges (when $\lambda_{GC} \sim b$). Figure 4D shows the adsorption of an ensemble of fully charged random chains and random chains with $f = 0.1$. Again, the adsorption behaves as expected with the fully charged chain adsorbing more and at lower surface charges. It is worth noticing once more that there is no qualitative differences between the adsorption of chains with different f.

In Figure 4 the effect of the chain length on the adsorption behavior is also depicted. The transition between high and low adsorption occurs at higher λ_{GC} for longer chains, which indicates that longer chains are more easily polarized by the electrical field from the wall.

To check the mean-field theories, for ensembles of chains with random sequences, the thickness of the adsorbed chains, $\langle z^2 \rangle^{1/2}$, is plotted against λ_{GC} in Figure 5. In Figure 5, 100 different sequences have been

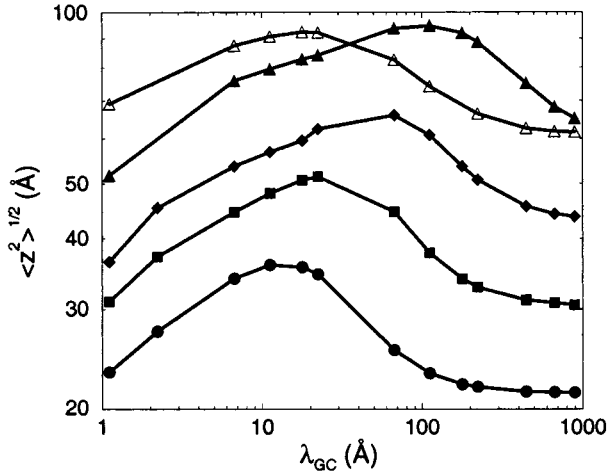

Figure 5. Thickness of the adsorbed layer as a function of λ_{GC} for chains with $N = 20$ (circles), $N = 40$ (squares), $N = 80$ (diamonds), and $N = 160$ (triangles), all with $f = 1.0$. The unfilled triangles correspond to $N = 160$ and $f = 0.1$.

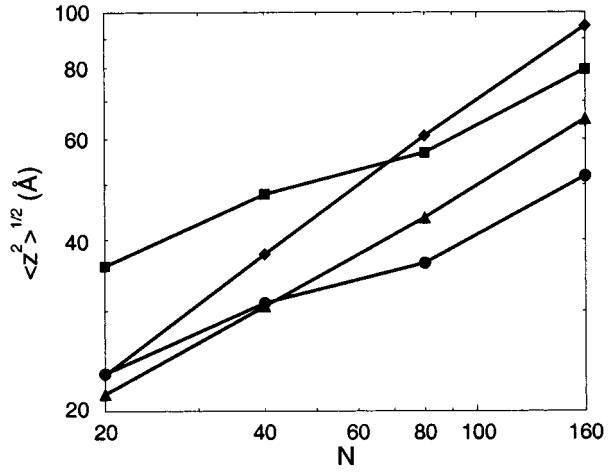

Figure 6. Thickness of the adsorbed layer as a function of chain size, for different surface charges: $\lambda_{GC} = 1.12$ Å (circles), $\lambda_{GC} = 11.2$ Å (squares), $\lambda_{GC} = 112$ Å (diamonds), and $\lambda_{GC} = 892$ Å (triangles).

simulated for every point plotted; i.e., for every N and λ_{GC} there are 100 simulations, and Figure 5 contains a total of 6200 simulations, which explains the necessity to use the simple and fast mean-field simulations.

For high λ_{GC} the chains do not adsorb, and $\langle z^2 \rangle^{1/2}$ approaches the bulk value $b\sqrt{(N-1)}/3$. In Figure 5, $\langle z^2 \rangle^{1/2}$ is actually somewhat smaller since the averaging is taken over a distance $b\sqrt{(N-1)}$ out from the wall, and in that range the chain dimension is disturbed by the wall. As adsorption sets in for lower λ_{GC}, $\langle z^2 \rangle^{1/2}$ starts to grow, but not with the predicted scaling relations given in Table 1. When $\langle z^2 \rangle^{1/2}$ reaches the same order of magnitude as λ_{GC}, $\langle z^2 \rangle^{1/2}$ hits a maximum and starts to decrease. The decrease does not follow the scaling relations shown in Table 1, though.

Figure 6 depicts how $\langle z^2 \rangle^{1/2}$ scales with N. For low surface charges, when the polyampholyte is in the bulk, the normal Gaussian scaling is retrieved $\langle z^2 \rangle^{1/2} \sim N^{0.5}$. For lower λ_{GC}, in what Dobrynin et al.[14] would call the pole regime there appears to be a scaling relation $\langle z^2 \rangle^{1/2} \sim N^{0.7}$, which is different from the ones predicted in Table 1, where $\langle z^2 \rangle^{1/2} \sim N^{3/2}$. For even higher surface charges there seems to be no simple scaling relationships. The scaling theories predict that in the fence and pancake regimes the size of the adsorbed chains will be independent of N, which is contradicted by the simulation results in Figure 6. Also, the claimed universality of the pancake regime where $\langle z^2 \rangle^{1/2} \approx b$ is not found in the simulations.

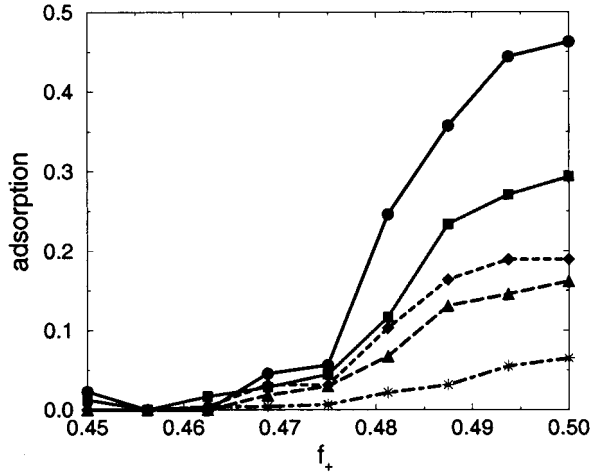

Figure 7. Adsorption of polyampholytes with a net negative charge to a negatively charged surface. The simulations have been carried out for chains with $N = 160$. Note that all monomers were charged and that the same 10 sequences have been used for the different Gouy−Chapman lengths which are $\lambda_{GC} = 2.2$ Å (circles), $\lambda_{GC} = 4.4$ Å (squares), $\lambda_{GC} = 6.6$ Å (diamonds), $\lambda_{GC} = 8.8$ Å (triangles), and $\lambda_{GC} = 22$ Å (stars).

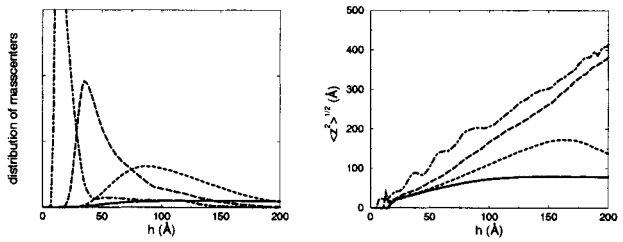

Figure 8. Distribution functions for (A) the mass centers and (B) for $\langle z^2 \rangle^{1/2}$. Averages over 100 random sequence chains with $N = 160$. The following Gouy−Chapman lengths have been used: $\lambda_{GC} = 1.12$ Å (dot−dashed lines), $\lambda_{GC} = 11.2$ Å (long-dashed lines), $\lambda_{GC} = 112$ Å (dashed lines), and $\lambda_{GC} = 892$ Å (solid lines).

The MC results and the scaling theories do not produce the same scaling exponents though the general trends coincide; i.e., $\langle z^2 \rangle^{1/2}$ increases with λ_{GC} until $\langle z^2 \rangle^{1/2} \approx \lambda_{GC}$, and then $\langle z^2 \rangle^{1/2}$ decreases with λ_{GC}.

3.2. Chains with a Net Charge. The interaction between polyampholytes with a net-negative charge and a negatively charged wall has been simulated. The results, given in Figure 7, confirm the results from the mean-field analysis[14,16] that the chains will adsorb and that the adsorption is stronger for higher surface charges. This is also reflected qualitatively in experiments.[12,23]

3.3. The Adsorption Mechanism. From the numerical simulations a wealth of information can be retrieved, which helps us to understand the adsorption behavior. In Figure 8A the distribution of mass centers is shown for different surface charges. It is clear that the chain moves closer to the surface at higher surface charges. The averaging over 100 chains means that different chains may contribute to different parts of the curve. In Figure 8B, the corresponding distribution for $\langle z^2 \rangle^{1/2}$ is given, i.e., the size that the average chain would have if it was positioned at a certain h. In Figure 5 the

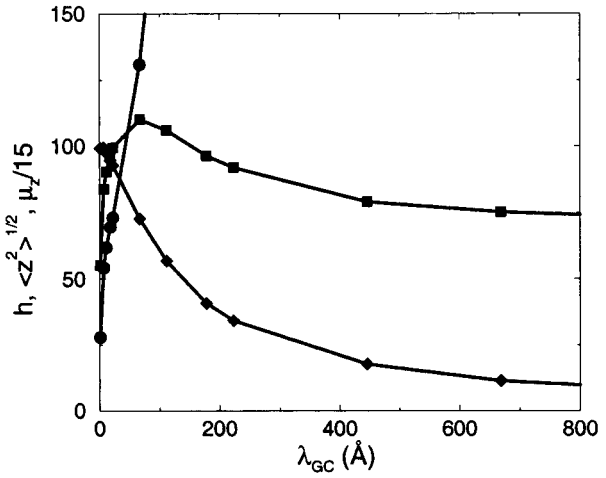

Figure 9. Distance to the wall for the polyampholyte mass centers h (circles), the size of the adsorbed layer $\langle z^2\rangle^{1/2}$ (squares), and the z-component of the dipole moment μ_z (diamonds) as a function of λ_{GC}. The curves are averages over 100 random sequence chains with $N = 160$. Note that the integration is over the full system in order to generate meaningful values of h.

size of the adsorbed chains is obtained as a convolution of the curves in Figure 8B with the corresponding curves in Figure 8A. Notice that even if high surface charges gives large $\langle z^2\rangle^{1/2}$ at around 200 Å from the surface, the chain will rarely occur at this position, and that part of the curve will not contribute to the mean value of $\langle z^2\rangle^{1/2}$ for the adsorbed chains. In Figure 8B this is also manifested in the poor averages for large h at high surface charges. The form of the distribution functions in Figure 8 shows why the choice of cutoff does not much alter the averages for the adsorbed chains. For high surface charges all of the chains are adsorbed and are well inside the cutoff, and for low surface charges $\langle z^2\rangle^{1/2}$ does not change much with h. Also, in Figure 9 the integration is taken over the full slit, and the results are not changed qualitatively.

In Figure 9, h, $\langle z^2\rangle^{1/2}$, and μ_z are shown as a function of λ_{GC}. The Monte Carlo simulations show that when the surface charge is increased a polyampholyte is drawn closer to the wall, and the chain responds to the increased electrical field by ordering its charges to increase the dipole strength, even if $\langle z^2\rangle^{1/2}$ decreases.

4. Conclusions

Monte Carlo simulations show that neutral polyampholytes adsorb to a charged surface. Also, a net charged chain can adsorb to a like charged surface. The adsorption increases with the surface charge, the polymer size, and the "broadness" of the charge distribution, with the diblock as one extreme.

For large λ_{GC} there is no adsorption, and the polyampholyte prefers the bulk. As λ_{GC} decreases, adsorption sets in and the chain expands. When λ_{GC} reaches the same magnitude as the chain dimension, the chain starts to contract. The size of the chains varies smoothly as described by Figure 5, and with decreasing λ_{GC} the chain is drawn closer to the wall and arranges its charges to increase the dipole strength. Furthermore, there exists no low-λ_{GC} region where all the oppositely charged monomers reside inside the Gouy−Chapman length as a flat pancake. The three distinct regions suggested from mean-field analysis are not reproduced in the numerical simulations, and it seems too bold to make pictures of the polyampholytes as pancakes, fences, and poles. However, MC and scaling theories do describe the same general behavior of the polyampholytes; i.e., even though the numbers of the exponents do not coincide, their signs appear to agree.

References and Notes

(1) Kudaibergenov, S. E. *Adv. Polym. Sci.* **1999**, *144*, 115−197.
(2) Ohlemacher, A.; Candau, F.; Munch, J. P.; Candau, J. *J. Polym. Sci., Polym. Phys. Ed.* **1996**, *34*, 2747−2757.
(3) Bratko, D.; Chakraborty, A. K. *J Phys. Chem.* **1996**, *100*, 1164−1173.
(4) Srivastava, D.; Muthukumar, M. *Macromolecules* **1996**, *29*, 2324−2326.
(5) Tanaka, M.; Grosberg, A. Y.; Tanaka, T. *J. Chem. Phys.* **1999**, *110*, 8176−8188.
(6) Wittmer, J.; Johner, A.; Joanny, J. F. *Europhys. Lett.* **1993**, *24*, 263−268.
(7) Pande, V. S.; Grosberg, A. Y.; Joerg, C.; Kardar, M.; Tanaka, T. *Phys. Rev. Lett.* **1996**, *77*, 3565−3568.
(8) Dobrynin, A. V.; Rubinstein, M. *J. Phys. II* **1995**, *5*, 677−695.
(9) Kantor, Y.; Kardar, M. *Phys. Rev. E* **1995**, *51*, 1299−1311.
(10) Soddeman, T.; Schiessel, H.; Blumen, A. *Phys. Rev. E* **1998**, *57*, 2081−2089.
(11) Dickinson, E. *Curr. Opin. Colloid Interface Sci.* **1998**, *3*, 633.
(12) Neyret, S.; Ouali, L.; Candau, F.; Pefferkorn, E. *J. Colloid Interface Sci.* **1995**, *176*, 86−94.
(13) Joanny, J. F. *J. Phys. II* **1994**, *4*, 1281−1288.
(14) Dobrynin, A. V.; Rubinstein, M.; Joanny, J.-F. *Macromolecules* **1997**, *30*, 4332−4341.
(15) Dobrynin, A. V.; Rubinstein, M.; Joanny, J.-F. *J. Chem. Phys.* **1998**, *109*, 9172−9176.
(16) Netz, R.; Joanny, J.-F. *Macromolecules* **1998**, *31*, 5123−5141.
(17) Engström, S.; Wennerström, H. *J. Phys. Chem.* **1978**, *82*, 2711.
(18) Israelachvili, J. *Intermolecular and Surface Forces*, 2nd ed.; Academic Press: London, 1991.
(19) Metropolis, N. A.; Rosenbluth, A. W.; Rosenbluth, M. N.; Teller, A.; Teller, E. *J. Chem. Phys.* **1953**, *21*, 1087−1097.
(20) Allen, M. P.; Tildesley, D. J. *Computer Simulation of Liquids;* Oxford University Press: Oxford, 1989.
(21) Imbert, J. B.; Victor, J. M.; Tsunekawa, N.; Hiwatari, Y. *Phys. Lett. A* **1999**, *268*, 92−98.
(22) Irbäck, A.; Peterson, C.; Potthast, F. *Proc. Natl. Acad. Sci. U.S.A.* **1996**, *93*, 9533−9538.
(23) Kamiyama, Y.; Israelachvili, J. *Macromolecules* **1992**, *25*, 5081−5088.

MA001437U